

This is an Open Access document downloaded from ORCA, Cardiff University's institutional repository:<https://orca.cardiff.ac.uk/id/eprint/161661/>

This is the author's version of a work that was submitted to / accepted for publication.

Citation for final published version:

Androvitsaneas, Petros , Clark, Rachel N., Jordan, Matthew, Alvarez Perez, Miguel, Peach, Tomas, Thomas, Stuart, Shabbir, Saleem, Sobiesierski, Angela D., Trapalis, Aristotelis, Farrer, Ian A. and Langbein, Wolfgang W. 2023. Direct-write projection lithography of quantum dot micropillar single photon sources. Applied Physics Letters

Publishers page:

Please note:

Changes made as a result of publishing processes such as copy-editing, formatting and page numbers may not be reflected in this version. For the definitive version of this publication, please refer to the published source. You are advised to consult the publisher's version if you wish to cite this paper.

This version is being made available in accordance with publisher policies. See <http://orca.cf.ac.uk/policies.html> for usage policies. Copyright and moral rights for publications made available in ORCA are retained by the copyright holders.



Direct-write projection lithography of quantum dot micropillar single photon sources

Petros Androvitsaneas,^{1,2} Rachel N. Clark,^{1,2} Matthew Jordan,^{1,2} Miguel Alvarez Perez,^{1,2} Tomas Peach,³ Stuart Thomas,³ Saleem Shabbir,³ Angela D. Sobiesierski,³ Aristotelis Trapalis,⁴ Ian A. Farrer,^{4,5} Wolfgang W. Langbein,⁶ and Anthony J. Bennett^{1,2,6}

¹*School of Engineering, Cardiff University, Queen's Buildings, The Parade, Cardiff, CF24 3AA, UK*

²*Translational Research Hub, Maindy Road, Cardiff, CF24 4HQ, UK*

³*Institute for Compound Semiconductors, Cardiff University, Queen's Buildings, The Parade, Cardiff, CF24 3AA, UK.*

⁴*Department of Electronic and Electrical Engineering, University of Sheffield, Mappin Street, S1 3JD, Sheffield, UK.*

⁵*EPSRC National Epitaxy Facility, University of Sheffield, Sheffield, S3 7HQ, UK.*

⁶*School of Physics and Astronomy, Cardiff University, Queen's Buildings, The Parade, Cardiff, CF24 3AA, UK.*

(*Electronic mail: BennettA19@cardiff.ac.uk)

(Dated: 11 August 2023)

We have developed a process to mass-produce quantum dot micropillar cavities using direct-write lithography. This technique allows us to achieve mass patterning of high-aspect ratio pillars with vertical, smooth sidewalls maintaining a high quality factor for diameters below 2.0 μm . Encapsulating the cavities in a thin layer of oxide (Ta_2O_5) prevents oxidation in the atmosphere, preserving the optical properties of the cavity over months of ambient exposure. We confirm that single dots in the cavities can be deterministically excited to create high-purity indistinguishable single photons with interference visibility (0.941 ± 0.008).

Single photon sources are an essential building block for a variety of quantum technologies¹. Developments in resonant excitation^{2,3}, in-situ lithography^{3,4} and cavity design^{5,6} have made quantum dots (QDs) one of the main contenders for high-efficiency and high-indistinguishability single photon sources. Furthermore, the potential to entangle photons sequentially emitted by the QDs using spin opens up new functionality in entangled photon pair generation⁷⁻¹⁰, cluster state generation¹¹ and other higher-dimensional photonic states^{12,13}.

One of the most promising cavity designs is the semiconductor micropillar cavity^{3,14,15} in which two distributed Bragg reflectors (DBRs) surround a spacer layer containing a low density layer of quantum dots. When etched into circular pillars of approximately 2 μm diameter these structures confine localised optical modes that enhance photon emission from the QDs, whilst coupling efficiently to a Gaussian-like mode that can be collected in the far field. A key challenge is achieving a deep vertical etch; this requires balancing the chemical and mechanical properties of the etch to manage the rate of re-deposition and minimise damage to the mask layer. Furthermore, the etched pillar sides must be smooth to limit the scattering loss and maintain a high quality factor (Q) and light collection efficiency. Therefore, fabrication requires a hard mask able to withstand the aggressive etch needed to remove up to 10 μm of semiconductor, but which is thin enough to be patterned with the necessary high accuracy. Different approaches to masking for this purpose have been demonstrated, including randomly positioned sapphire nanocrystals¹⁶, contact lithography with a quartz mask¹⁷, electron beam lithography¹⁸ and cryogenic in-situ laser-lithography⁴. The latter two allow for pre-selection of promising QDs and alignment

of cavities, but are expensive and less compatible with mass production of devices.

Here we report a direct-write photolithography method allowing high-throughput sample patterning for deep etches of GaAs. This technique, also known as mask-less lithography, uses a UV light source and a digital light modulator to project the pattern onto the sample, with potential to reconfigure designs by software. It provides the flexibility of electron beam lithography, at a lower cost, and with a 400 nm resolution that is sufficient for this application. Characterisation of the cavities show they have low sidewall scattering parameters, retaining high Q -factors even at low diameters. Finally, we demonstrate a high brightness, high purity and indistinguishable single photon source using deterministic pulsed resonant excitation, to verify the quality of the material.

The samples were grown by molecular beam epitaxy with $\sim 0.5\%$ variation in growth rate over the 3-inch wafer, resulting in a uniform dot density. A high Q cavity sample was grown consisting of a lower Bragg mirror of 26 pairs of alternating $\text{Al}_{0.95}\text{Ga}_{0.05}\text{As}$ ¹⁹ and GaAs $\lambda/4$ layers, a single wavelength spacer with InAs QDs at its center, and a final 17 pair Bragg mirror. A low Q cavity was also grown with 7/26 Bragg mirror pairs, both with a design wavelength of 940 nm. The processing proceeds as shown in Fig. 1 (a) by coating the chips with a hard-mask layer of 750 nm SiO_2 deposited via plasma enhanced chemical vapour deposition (PECVD). A 2 μm layer of negative photo-resist, AZ2020, is applied and exposed using the MicroWriter ML3 Pro direct-write photolithography tool. The pattern consists of discs with diameters in the range 1.55 μm to 5.00 μm in regularly spaced 5×5 arrays. This direct-write method allows for the patterning of 14,000 devices in 240 s, which we estimate is two orders of

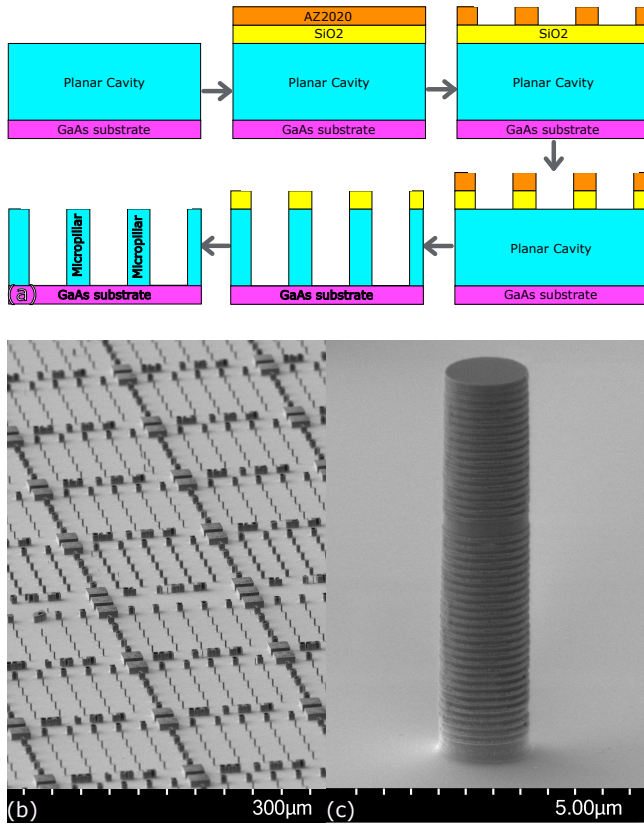


FIG. 1. Micropillar fabrication. (a) Schematic of processing steps. (b) Wide area scanning electron microscope image (SEM) of etched structures with a variety of different diameters. (c) SEM of a high Q -factor micropillar of diameter $1.75 \mu\text{m}$

magnitude faster than electron beam lithography. After developing the photoresist in AZ726, the hard mask is etched using a $\text{C}_4\text{F}_8/\text{O}_2$ inductively coupled plasma (ICP) and the photoresist removed. The semiconductor is then etched using a $\text{Cl}_2/\text{BCl}_3/\text{N}_2$ ICP and the hard mask is then removed with a second $\text{C}_4\text{F}_8/\text{O}_2$ etch. Finally, the micropillars are encapsulated in a 10 nm layer of Ta_2O_5 using atomic layer deposition. This oxide layer provides a uniform conformal coating that protects the samples against oxidation, especially for the DBR layers containing aluminium⁵. Between 1 and 2 cavities out of 200 micropillars with diameters below $2 \mu\text{m}$ are critically damaged and display no emission at all, not even off-resonant feeding of the cavity mode. Amongst the remaining majority which show some emission, the overall yield of micropillars with sharp QD emission lines within the FWHM of the cavity mode is 0.5% for a high Q -factor sample. All cavities in the low Q sample have such lines within the mode, as a result of the rather high areal density of dots.

The quality of the patterning and semiconductor etch determines the sidewall roughness, which introduces losses to the cavity mode HE_{11} ¹⁸. The overall loss rate for photons in the mode is inversely proportional to the quality factor at a given diameter, $1/Q(d) = 1/Q_0 + 1/Q_s(d)$, where the decay rate due to sidewall roughness is parameterized by $1/Q_s(d)$, which adds to the loss rate through mirrors $1/Q_0$. Q_0 can

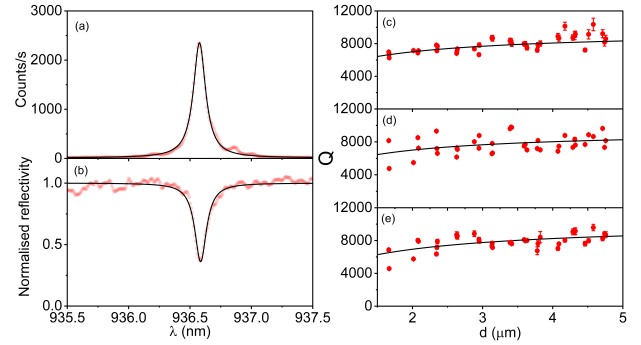


FIG. 2. Cavity quality factors. (a) Photoluminescence (PL) spectrum of the cavity mode (red data points) with the corresponding Lorentzian fit (black line) of a micropillar consisting of 17/26 period Bragg mirrors and a diameter $d = 3.14 \mu\text{m}$ at 80 K, yielding a $Q = 7740 \pm 60$. (b) Normalised white light reflectivity (WLR) (red data points) for the same micropillar at 80 K with the Lorentzian fit (black line), yielding a $Q = 8100 \pm 300$. (c) $Q(d)$ measured at 4 K by WLR (d) $Q(d)$ measured at 80 K by PL and (e) by WLR. Fits shown as black lines discussed in the text.

be determined from the Q -factor that cavities tend towards at high diameter. $Q_s(d)$ is linked to the diameter of the micropillar by the following expression $1/Q_s(d) = 2k_s J_0^2(kd/2)/d$, where k_s is the sidewall loss coefficient, $J_0(kd/2)$ is the 0th order Bessel function with k the transverse wavevector and d the diameter¹⁸.

The high Q -factor structure allows us to measure any losses resulting from sidewall roughness created during the lithography and etch processes. Two different techniques have been utilised to measure the cavity's $Q(d)$, photoluminescence (PL) and white light reflectivity (WLR), with example data shown in Fig. 2(a) and (b). The relatively high density of spectrally sharp QD transitions in the spectral range of the mode, made the measurement of Q using PL at 4 K unreliable. Therefore, the WLR measurement was used to determine the Q -factor of HE_{11} at this temperature, Fig. 2(c). Additionally, we measure the Q -factors at 80 K using PL (Fig. 2(d)) and WLR (Fig. 2(e)). All three datasets yield a similar value for the sidewall loss coefficient k_s , (c) k_s of (48 ± 9) pm, (d) (50 ± 20) pm and (e) (60 ± 20) pm. These values are comparable to the state-of-the-art for these photonic structures¹⁸ which reports $k_s = 68$ pm. The Q -factor of the $1.85 \mu\text{m}$ cavity is approximately one third of the value estimated in our simulations, suggesting the maximum Purcell Factor that could be observed would be similarly reduced, to a value of 25.

In the course of our studies we have confirmed dots in both cavity designs display antibunching to a few % level under weak resonant CW excitation, as expected^{17,20}. Several previous reports have shown highly indistinguishable (> 0.9 visibility) quantum light emission under pulsed resonant excitation in pillar cavities of comparable high Q , where the reduction in radiative lifetime is expected to improve the indistinguishability^{3,6,14}. More surprisingly, we find that the quality of the dots in this material is sufficient to generate highly indistinguishable photons under resonant excitation with only a modest Purcell factor of ~ 3 in a low Q sample. The sample was

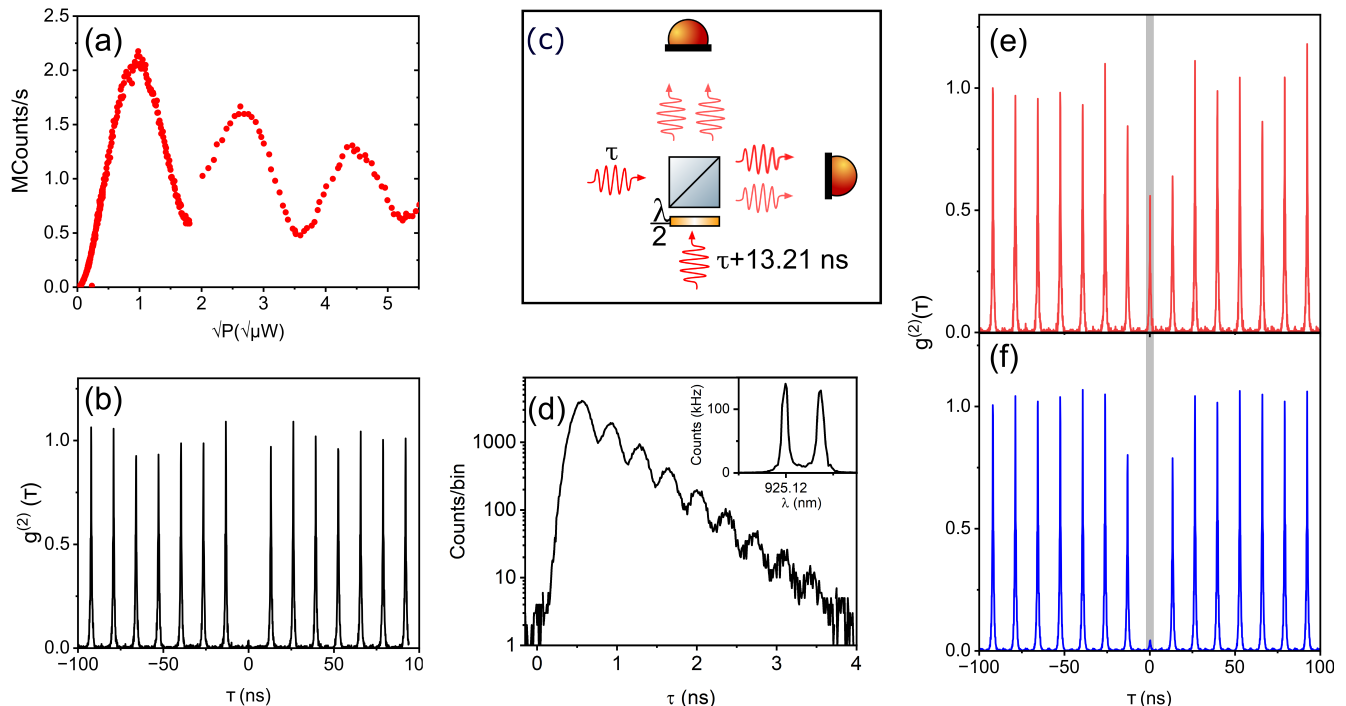


FIG. 3. Indistinguishable single photons from a deterministically driven neutral exciton transition in a micropillar. (a) Rabi oscillation in pulse amplitude for a neutral exciton in a 7/26 period Bragg mirror cavity, the discontinuity at the point of 2π stems from the measurement using a neutral density filter to allow the two power ranges. (b) Pulsed $g^{(2)}(\tau)$ produced by fully inverting the system using a π -pulse, at a power of $0.969 \sqrt{\mu\text{W}}$, with $g^{(2)}(0) = 0.027 \pm 0.004$. (c) Setup used to interfere two subsequent photons generated 13.2 ns apart. A half waveplate ($\lambda/2$) is used to introduce polarization indistinguishability. The interferometer used had a first order visibility of 0.950 ± 0.002 , characterised with a narrow (< 1 MHz) single frequency laser at the same approximate wavelength. (d) time resolved emission intensity after a short pulse showing a beat which arises from the exciton's fine structure splitting (shown in CW laser resonance fluorescence spectral scan, inset). (e) Hong-Ou-Mandel interference measurement for orthogonally polarized photons and (f) co-polarized photons. The visibility is 0.889 ± 0.006 , derived by the ratio of the areas denoted by the shaded rectangle. Correlations are normalized by the mean area at large delays. Accounting only for multi-photon emission from the source, $g^{(2)}(0)$, the inferred indistinguishability is 0.941 ± 0.008 .

stored in air for three months after the processing with no observable degradation in Q or emission. It has been shown that these low Q cavities can be efficient and broadband^{21,22}. A standard dark field microscope setup is used²⁰ in which the input can be swapped between laser excitation and a broadband light emitting diode for reflectivity. The cross-polarized resonantly scattered light is collected into a polarisation maintaining fiber and directed to a spectrometer or superconducting nanowire single photon detectors (SNSPDs). Optical losses, polarization filtering, and SNSPD detector efficiency combine to give an overall system efficiency of $(4.5 \pm 0.6)\%$.

We study a neutral exciton on resonance with the HE_{11} in a $1.7 \mu\text{m}$ diameter micropillar with a low Q -factor ($Q = 440 \pm 30$) and 7/26 Bragg mirror pairs. This exciton displays a fine structure splitting of $11 \mu\text{eV}$ and the corresponding beat is observed within the radiative decay time of 480 ps. Finite-difference time-domain (FDTD) simulations performed using Ansys Lumerical²³ using a horizontal electric dipole at the center of the cavity, driven as a pulse of 5.6 ps duration over a spectral range from 845 nm to 1060 nm and at the frequency of the HE_{11} mode, reveal a maximum Purcell factor of 3.16 with an overall expected efficiency of up to 0.79 at the collection objective above the pillar. Measurements of a control sample

with similar dots and no cavity reveal a mean radiative lifetime of 1.30 ns, which indicates the transition reported here has a Purcell factor of 2.70.

Exciting the transition resonantly in a cross-polarized geometry²⁰ we vary the pulse amplitude to observe a Rabi oscillation. With π -pulse excitation the maximum count-rate is ~ 2.2 MHz, measured by an SNSPD, see Fig. 3(a), which corresponds to a “first lens brightness” of 64%. A second order autocorrelation measurement reveals the purity of the single photon emission²⁴, when the system undergoes a full population inversion under the excitation of π -pulse, to give $g^{(2)}(0) = 0.027 \pm 0.004$, see Fig. 3(b).

Finally, we measure the indistinguishability of the single photons emitted under the conditions described above by interfering two sequentially emitted photons from the QD, Fig. 3(c). This yields a raw visibility of the two-photon interference 0.889 ± 0.006 Fig. 3(d-e). We infer the indistinguishability value by accounting for the finite $g^{(2)}(0)$ to be 0.941 ± 0.008 ²⁵. This value is comparable to the visibility achieved with QDs in cavities with higher Purcell factors^{1,3,5,14,15}. This shows the excellent condition of the material even after the prolonged exposure to a non-controlled atmosphere. In the course of preparing this manuscript we mea-

TABLE I. Performance metrics of 5 sources in the sample.

λ (nm)	Rate (MHz) ^a	$g^{(2)}(0)$	HOM visibility ^b	Lifetime (ps)
925.12 ^c	2.2	0.027	0.941	480
925.35	2.1	0.021	0.920	474
924.62	1.6	0.028	0.907	449
925.35	0.9	0.044	0.916	471
925.91	1.5	0.066	0.932	545

^a under π -pulse excitation

^b Recorded under π -pulse excitation and corrected for finite $g^{(2)}(0)$

^c this is the dot discussed in Fig. 3

sured similar results on a number of dots, which is summarized in Table I. This shows the reproducibility of the results in cavities on the same chip, albeit with the inherent bias of pre-selecting transitions that are spectrally isolated and bright under non-resonant excitation.

This direct-write method can be used for high-volume manufacturing of QD micropillar devices. The quality of the structure, low sidewall roughness, and high-purity of the indistinguishable photons, shows its promise as a flexible platform for mass production of single photon sources. Future work could improve the collection efficiency into a single mode fiber by optimizing the far field emission pattern. An increased yield of optimized structures could be achieved by mapping the locations of dots prior to the processing, facilitating the repositioning of cavities and dots over a whole chip without the need for cryogenic lithography⁴. Furthermore, with positioned arrays of QDs becoming available²⁶, the yield could approach unity.

ACKNOWLEDGMENTS

We acknowledge financial support provided by EPSRC via Grant No. EP/T017813/1 and EP/T001062/1. RC was supported by grant EP/S024441/1, Cardiff University and the National Physical Laboratory (NPL). We thank Alastair Sinclair and Philip Dolan at NPL, and David Ellis at the Cavendish Laboratory for technical discussions. Device processing was carried out in the cleanroom of the ERDF-funded Institute for Compound Semiconductors (ICS) at Cardiff University. For the purpose of open access, the author has applied a CC BY public copyright licence.

DATA AVAILABILITY STATEMENT

The data that support the findings of this study are openly available in the Cardiff University Research Portal at <http://doi.org/10.17035/d.2023.0257041928>.

REFERENCES

- Y. Arakawa and M. J. Holmes, *Applied Physics Reviews* **7**, 021309 (2020).
- E. B. Flagg, A. Muller, J. Robertson, S. Founta, D. Deppe, M. Xiao, W. Ma, G. Salamo, and C.-K. Shih, *Nature Physics* **5**, 203 (2009).
- N. Somaschi, V. Giesz, L. De Santis, J. Loredo, M. P. Almeida, G. Hornecker, S. L. Portalupi, T. Grange, C. Anton, J. Demory, *et al.*, *Nature Photonics* **10**, 340 (2016).
- A. Dousse, L. Lanco, J. Suffczyński, E. Semenova, A. Miard, A. Lemaître, I. Sagnes, C. Roblin, J. Bloch, and P. Senellart, *Physical review letters* **101**, 267404 (2008).
- N. Tomm, A. Javadi, N. O. Antoniadis, D. Najer, M. C. Löbl, A. R. Korsch, R. Schott, S. R. Valentin, A. D. Wieck, A. Ludwig, *et al.*, *Nature Nanotechnology* **16**, 399 (2021).
- Y.-M. He, Y. He, Y.-J. Wei, D. Wu, M. Atatüre, C. Schneider, S. Höfling, M. Kamp, C.-Y. Lu, and J.-W. Pan, *Nature nanotechnology* **8**, 213 (2013).
- R. M. Stevenson, R. J. Young, P. Atkinson, K. Cooper, D. A. Ritchie, and A. J. Shields, *Nature* **439**, 179 (2006).
- R. J. Young, R. M. Stevenson, P. Atkinson, K. Cooper, D. A. Ritchie, and A. J. Shields, *New Journal of Physics* **8**, 29 (2006).
- A. Dousse, J. Suffczyński, A. Beveratos, O. Krebs, A. Lemaître, I. Sagnes, J. Bloch, P. Voisin, and P. Senellart, *Nature* **466**, 217 (2010).
- F. B. Basset, M. B. Rota, C. Schimpf, D. Tedeschi, K. D. Zeuner, S. C. Da Silva, M. Reindl, V. Zwiller, K. D. Jöns, A. Rastelli, *et al.*, *Physical Review Letters* **123**, 160501 (2019).
- I. Schwartz, D. Cogan, E. R. Schmidgall, Y. Don, L. Gantz, O. Kenneth, N. H. Lindner, and D. Gershoni, *Science* **354**, 434 (2016).
- J. P. Lee, B. Villa, A. J. Bennett, R. M. Stevenson, D. J. P. Ellis, I. Farrer, D. A. Ritchie, and A. J. Shields, *Quantum Science and Technology* **4**, 025011 (2019).
- M. H. Appel, A. Tiranov, S. Pabst, M. L. Chan, C. Starup, Y. Wang, L. Midolo, K. Tiurev, S. Scholz, A. D. Wieck, *et al.*, *Physical Review Letters* **128**, 233602 (2022).
- X. Ding, Y. He, Z. C. Duan, N. Gregersen, M. C. Chen, S. Unsleber, S. Maier, C. Schneider, M. Kamp, S. Höfling, C.-Y. Lu, and J.-W. Pan, *Physical Review Letters* **116**, 020401 (2016).
- H. Wang, Y.-M. He, T.-H. Chung, H. Hu, Y. Yu, S. Chen, X. Ding, M.-C. Chen, J. Qin, X. Yang, R.-Z. Liu, Z.-C. Duan, J.-P. Li, S. Gerhardt, K. Winkler, J. Jurkat, L.-J. Wang, N. Gregersen, Y.-H. Huo, Q. Dai, S. Yu, S. Höfling, C.-Y. Lu, and J.-W. Pan, *Nature Photonics* **13**, 770 (2019).
- C. Santori, D. Fattal, J. Vučković, G. S. Solomon, and Y. Yamamoto, *Nature* **419**, 594 (2002).
- A. J. Bennett, J. P. Lee, D. J. P. Ellis, I. Farrer, D. A. Ritchie, and A. J. Shields, *Nature Nanotechnology* **11**, 857 (2016).
- C. Schneider, P. Gold, S. Reitzenstein, S. Höfling, and M. Kamp, *Applied Physics B* **122**, 19 (2016).
- N. Cho, K. Kim, J. Song, W. Choi, and J. Lee, *Solid State Communications* **150**, 1955 (2010).
- A. V. Kuhlmann, J. Houel, D. Brunner, A. Ludwig, D. Reuter, A. D. Wieck, and R. J. Warburton, *Review of Scientific Instruments* **84**, 073905 (2013).
- P. Androvitsaneas, A. B. Young, C. Schneider, S. Maier, M. Kamp, S. Höfling, S. Knauer, E. Harbord, C. Y. Hu, J. G. Rarity, and R. Oulton, *Physical Review B* **93**, 241409 (2016).
- L. Ginés, M. Moczala-Dusanowska, D. Dłaka, R. Hošák, J. R. Gonzales-Ureta, J. Lee, M. Ježek, E. Harbord, R. Oulton, S. Höfling, *et al.*, *Physical Review Letters* **129**, 033601 (2022).
- Ansys Lumerical: Purcell factor of a microdisk: <https://optics.ansys.com/hc/en-us/articles/360041612594-Purcell-factor-of-a-microdisk> (2023).
- R. H. Brown and R. Q. Twiss, *The London, Edinburgh, and Dublin Philosophical Magazine and Journal of Science* **45**, 663 (1954).
- H. Ollivier, S. Thomas, S. Wein, I. M. de Buy Wenniger, N. Coste, J. Loredo, N. Somaschi, A. Harouri, A. Lemaître, I. Sagnes, *et al.*, *Physical Review Letters* **126**, 063602 (2021).
- J. Große, M. von Helversen, A. Koulas-Simos, M. Hermann, and S. Reitzenstein, *APL Photonics* **5**, 096107 (2020).